JOURNAL OF VIROLOGY, Sept. 2005, p. 12016–12024 Vol. 79, No. 18
0022-538X/05/$08.00+0 doi:10.1128/JVI.79.18.12016–12024.2005

Inhibition of Coxsackie B Virus Infection by Soluble Forms of Its Receptors: Binding Affinities, Altered Particle Formation, and Competition with Cellular Receptors

Ian G. Goodfellow,[1,2] David J. Evans,[2] Anna M. Blom,[3] Dave Kerrigan,[2] J. Scott Miners,[4] B. Paul Morgan,[4] and O. Brad Spiller[4]*

School of Animal and Microbial Sciences, University of Reading, P.O. Box 228, Reading RG6 6AJ, United Kingdom[1]; Division of Virology, Institute of Biomedical and Life Sciences, University of Glasgow, Church Street, Glasgow G11 5JR, United Kingdom[2]; Department of Laboratory Medicine, Lund University, University Hospital Malmö, Malmö S-20502, Sweden[3]; and Department of Medical Biochemistry and Immunology, School of Medicine, Cardiff University, Henry Wellcome Building, 3rd floor, Heath Park, Cardiff CF14 4XN, United Kingdom[4]

Received 7 January 2005/Accepted 13 June 2005

We previously reported that soluble decay-accelerating factor (DAF) and coxsackievirus-adenovirus receptor (CAR) blocked coxsackievirus B3 (CVB3) myocarditis in mice, but only soluble CAR blocked CVB3-mediated pancreatitis. Here, we report that the in vitro mechanisms of viral inhibition by these soluble receptors also differ. Soluble DAF inhibited virus infection through the formation of reversible complexes with CVB3, while binding of soluble CAR to CVB induced the formation of altered (A) particles with a resultant irreversible loss of infectivity. A-particle formation was characterized by loss of VP4 from the virions and required incubation of CVB3-CAR complexes at 37°C. Dimeric soluble DAF (DAF-Fc) was found to be 125-fold-more effective at inhibiting CVB3 than monomeric DAF, which corresponded to a 100-fold increase in binding affinity as determined by surface plasmon resonance analysis. Soluble CAR and soluble dimeric CAR (CAR-Fc) bound to CVB3 with 5,000- and 10,000-fold-higher affinities than the equivalent forms of DAF. While DAF-Fc was 125-fold-more effective at inhibiting virus than monomeric DAF, complement regulation by DAF-Fc was decreased 4 fold. Therefore, while the virus binding was a cooperative event, complement regulation was hindered by the molecular orientation of DAF-Fc, indicating that the regions responsible for complement regulation and virus binding do not completely overlap. Relative contributions of CVB binding affinity, receptor binding footprint on the virus capsid, and induction of capsid conformation alterations for the ability of cellular DAF and CAR to act as receptors are discussed.

Coxsackie B viruses (CVB) are enteroviruses belonging to the family *Picornaviridae* of single positive-stranded RNA viruses. All known serotypes of CVB use the coxsackievirus-adenovirus receptor (CAR) as a primary receptor to infect permissive cells (3, 4, 25). CAR is a member of the CTX immunoglobulin superfamily (8) and elucidation of its physiologic function is the focus of numerous investigators. Human CAR has been shown to be a component of homotypic intercellular contacts of nonpolarized cells and tight junctions in polarized cells (9), and mouse CAR has been identified as a candidate adhesion molecule in the developing mouse brain (19, 20). Affinity chromatography has also shown that human CAR binds to immunoglobulin G (IgG) and IgM, but the biological significance of this finding is currently unclear (7). CVB serotypes 1, 3, and 5 have additionally been found to bind decay-accelerating factor (DAF) as a coreceptor (4, 5, 17, 33). DAF is a member of the regulators of complement activation gene cluster and is well established as a potent complement regulator, as well as a ligand for numerous pathogens and the leukocyte activation marker CD97 (14, 24, 41).

* Corresponding author. Mailing address: Virus Receptor and Immune Evasion Group, School of Medicine, Cardiff University, Henry Wellcome Building, 3rd floor, Heath Park, Cardiff CF14 4XN, United Kingdom. Phone: 44 02920 742471. Fax: 44 02920 744001. E-mail: SpillerB@cardiff.ac.uk.

The relative dependence on DAF and CAR expression for CVB3 infection can be altered, depending on the cell line in which the virus is propagated. Where the target cells express both DAF and CAR, infection of low-passage clinical CVB isolates can be inhibited to various degrees with antibodies to either DAF or CAR (3, 25). While incubation of wild-type CVB strains with human fibroblasts or rhabdomyosarcoma cell lines (DAF positive, CAR negative) result in a nonlytic persistent carrier type infection (31, 34), some strains adapt after several passages and acquire the ability to lytically infect these cell lines (5, 31, 32). These resultant strains are characterized by high-affinity binding to DAF and the ability to hemagglutinate erythrocytes through DAF binding. However, the capacities of DAF and CAR to act as receptors and impart permissiveness to infection are not equivalent. Chinese hamster ovary (CHO) cells transfected with human CAR are fully permissive, and CVB infection results in subsequent cytolysis (3, 25, 31), while CHO cells transfected with human DAF will readily bind large quantities of CVB (36) but are not fully permissive to infection, even to the DAF-adapted strains (4, 5, 33, 40).

Recently, we reported that soluble recombinant Fc fusion forms of DAF and CAR can inhibit CVB-mediated myocarditis in mice (43, 44). However, CAR-Fc was found to additionally inhibit CVB-mediated pancreatitis, while DAF-Fc did not. To address these differences in CAR and DAF interactions with CVB in vivo, we have developed in vitro blocking assays

using soluble recombinant receptors. Given that the virus is likely to complex with multiple DAF and/or CAR molecules on the cell surface, the effect of valency on infection blocking efficacy was examined by comparing monomeric and dimeric forms of soluble DAF and CAR. The ability of soluble recombinant forms of CAR and DAF to cause reversible or irreversible CVB neutralization in vitro was also analyzed. To examine the biophysical basis of these differences, the binding kinetics to CVB were also elucidated for monomeric and dimeric forms of DAF and CAR by surface plasmon resonance (SPR) analysis.

MATERIALS AND METHODS

Virus strains. Defined CVB serotypes 1, 3, and 5, the kind gift of Brian Megson, Public Health Laboratory Service, Colindale, London, United Kingdom, were adapted to a rhabdomyosarcoma (RD) cell line through serial propagation. Cardiopathogenic CVB3 strains were generously provided by Charles Gauntt (University of Texas Health Sciences Center, San Antonio, TX), and Reinhard Kandolf (University of Tubingen, Tubingen, Germany), and these viruses were passaged in HeLa cells with regular inoculation and recovery from A/J mice.

Cell lines. Human RD and HeLa cells were obtained from the European Collection of Animal Cell Cultures, Porton Down, United Kingdom. The IBRS-2 (IBRS) pig kidney cell line was obtained from the American Type Culture Collection, Manassas, VA. Primary human foreskin fibroblasts (HuFF) were obtained by standard isolation procedures in-house. All cells were grown in Dulbecco's modified essential medium containing glutamine and penicillin-streptomycin and supplemented with 10% fetal calf serum (all purchased from GibcoBRL, Paisley, United Kingdom).

Soluble recombinant DAF and CAR. Construction, expression, and purification of the CVB receptors DAF and CAR, fused to the carboxy terminus of human IgG1 Fc (DAF-Fc and CAR-Fc), are described elsewhere (16, 44). Monomeric DAF was produced using a *Pichia pastoris* expression system as previously described (29). Monomeric CAR and DAF were also produced by proteolytic cleavage of purified Fc fusion proteins with papain-agarose (Sigma). Briefly, 10 mg of each protein was dialyzed into 20 mM phosphate–2 mM EDTA buffer (pH 7.4) and incubated with 50 μg of agarose-conjugated papain for 1 h on ice. Complete cleavage and integrity of released DAF and CAR fragments were investigated by silver-stained sodium dodecyl sulfate-polyacrylamide gel electrophoresis to ensure the correct molecular mass of resultant fragments. The papain-agarose was removed by centrifugation (10,000 × *g* for 3 min), and the supernatant containing the cleaved proteins was run over a ProSep-A column (Amersham) to remove the released Fc fragments. Column flowthrough and subsequent phosphate-buffered saline (PBS) washes containing only the released DAF or CAR were concentrated and buffer exchanged back into PBS by using an Amicon concentrator with a 10-kDa cutoff filter. Complete removal of Fc fragments and uncleaved protein was confirmed by Western blot analysis using the antibodies listed below. Protein concentration was determined by an enzyme-linked immunosorbent assay using monoclonal anti-DAF or anti-CAR antibodies (see below) to capture antigen and rabbit polyclonal antiserum raised against monomeric DAF or CAR to detect captured antigen. Plate-bound rabbit antibody was developed with horseradish peroxidase-conjugated goat anti-rabbit immunoglobulin antibody (Bio-Rad Laboratories) and detected with OPD tablets (DAKO) per the manufacturer's instructions. The concentration of standards was determined by an in-house acid hydrolysis method, and all stocks were standardized to 1 mg/ml.

Antibodies. Mouse monoclonal antibody (MAb) recognizing DAF (MBC1) was a gift of Claire Harris (Cardiff University), and the MAb anti-CAR antibody (BRAD30) was generated in-house. The hybridoma cell line OX23, secreting mouse monoclonal anti-human factor H, was obtained from the European Collection of Animal Cell Cultures and was used as the isotype-matched control for the mouse MAbs. Rabbit polyclonal antisera were raised against soluble recombinant human DAF and CAR in-house. Rabbit polyclonal antiserum raised against soluble HHV-8 open reading frame 4, also raised in-house, provided a control antibody for the rabbit polyclonal antiserum. Phycoerythrin-conjugated goat anti-mouse Ig secondary antibody was purchased from DAKO, Ltd. (Angel Drove, Ely, United Kingdom) and phycoerythrin-conjugated goat anti-rabbit Ig secondary antibody was purchased from Sigma Chemical Co. (Poole, United Kingdom). Horseradish peroxidase-conjugated goat anti-rabbit Ig secondary antibody was purchased from Bio-Rad Laboratories, Ltd. (Hemel Hempstead, United Kingdom).

Virus titration and blocking assays. A total of 10,000 cells of each cell line to be tested were seeded into each well of 96-well plates 24 h prior to infection. A 10-fold dilution series was made for each virus in ice-cold serum-free cell medium and then mixed with an equal volume of serum-free cell medium (control) or DAF-Fc or CAR-Fc (to a final concentration of 0.6 μM) in ice-cold serum-free cell medium. After the virus and inhibitor (or control) were allowed to complex on ice for 30 min, 100 μl per well of each test sample was overlaid on the cells and allowed to incubate for 72 h in a CO_2 cell incubator at 37°C. Viable cells were visualized after staining with 0.1% crystal violet–0.1% formaldehyde in PBS. Successful blockage of infection was observed as a blue cell layer at 3 days postinfection. All experiments were repeated several times to assure reproducibility of results. For experiments where inhibitor concentrations were varied, 10^4 infectious virus units in ice-cold serum-free medium (final concentration) were mixed with an equal volume containing (amounts specified in Results) CAR-Fc, DAF-Fc, monomeric CAR, monomeric DAF, or control medium prior to incubation on ice and treated as detailed above.

Radiolabeling CVB and purification of 160S particles. CVB was labeled with [^{35}S]methionine by prestarving a 95% confluent 75-cm^2 flask of HeLa or RD cells with serum-free, methionine-free cell medium (Sigma) for 2 h in the CO_2 cell incubator. Cells were then incubated with 10^9 50% tissue culture infective doses ($TCID_{50}$) of virus in 1 ml at room temperature with frequent rocking for 30 min, prior to removal of the inoculum and replacement of the methionine-free cell medium. After 2 h, the cell medium was replaced with serum-free, methionine-free cell medium containing 0.1 MBq [^{35}S]methionine (Amersham), and incubation continued overnight. Cell supernatant was cleared of cell debris by centrifugation at 1,000 × *g* for 3 min, and the virus-containing cell supernatant was filtered through a 0.2-μm syringe filter. Radiolabeled virus was pelleted through a 30% sucrose cushion at 40,000 × *g* overnight and then resuspended with a 27-gauge needle in PBS containing 0.1% bovine serum albumin (BSA). A 10 to 25% sucrose gradient was made using the BioComp gradient master (BioComp Instruments, Fredericton, Canada), and the full (160S), procapsid (135S), and empty (80S) capsids were separated by centrifugation on the gradient at 40,000 × *g* for 1 h 15 min, followed by fractionation. Virus strains CVB3-CG, RD, and H were successfully labeled, but attempts to radiolabel and purify CVB3-RK proved unsuccessful, as this virus was unstable during the purification process. Ten-microliter aliquots of each fraction were measured by scintillation counting to identify the radioactive peaks. Peak radioactive fractions corresponding to full capsids (160S) were then pooled, diluted twofold with PBS containing 0.1% BSA, pelleted at 50,000 × *g* for 2 h, and then resuspended in 200 μl of PBS-BSA.

CVB-receptor complex analysis. For neutralization assays, 100,000 cpm of each virus was incubated with 0.6 μM CAR-Fc or DAF-Fc, 10^8 permissive cells (RD cells for CVB3-RD; HeLa cells for the rest), or serum-free cell medium on ice for 1 h. For the permissive cell control, unbound virus was removed by three washes in ice-cold serum-free cell medium and then resuspended to the original volume. All samples (unless otherwise specified) were then incubated for 2 h at 37°C on a rotator. Insoluble debris and cells were then removed by centrifugation at maximum speed in a benchtop microfuge at 4°C for 10 min, then loaded on a 10 to 25% sucrose gradient, and separated as detailed above. Gradients were separated into 0.5-ml fractions, and 0.1 ml of each fraction was measured by scintillation counting to determine radioactivity. Each condition was repeated three times to ensure reproducibility of results. To determine residual infectivity of peak fractions, 0.1 ml was taken and dialyzed against PBS to remove sucrose and then used to infect cells to determine the $TCID_{50}$ as detailed above (without preincubation on ice or dilution with medium or inhibitors).

Detection of VP4. Viral capsid proteins from the sucrose gradient separations were precipitated by the addition of 1 ml of 10% trichloroacetic acid to 0.3 ml of the peak radioactive fractions on ice for 2 h; the precipitated proteins were then pelleted by centrifugation at 10,000 × *g* in a benchtop microfuge at 4°C. Protein pellets were washed once with 1 ml of ice-cold acetone and air dried before being dissolved in Tricine gel sample buffer and separating proteins on a 10% Tricine gel (Bio-Rad Laboratories). Gels were dried, and radioactive bands were visualized by phosphorimaging (Bio-Rad Laboratories).

Inhibition of classical pathway C3 convertase. Sheep erythrocytes were washed twice with $DGVB^{++}$ (2.5 mM veronal buffer, pH 7.3, 72 mM NaCl, 140 mM glucose, 0.1% gelatin, 1 mM $MgCl_2$, and 0.15 mM $CaCl_2$), suspended at a concentration of 10^9 cells/ml, and incubated for 20 min at 37°C with an equal volume of amboceptor (Boehring Diagnostics, Germany; diluted 1:3,000 in $DGVB^{++}$) to make EA cells. Purified complement components were purchased from Advanced Research Technologies (San Diego, Calif.). EAC1 cells were made by washing the EA cells twice with ice-cold $DGVB^{++}$ and resuspending

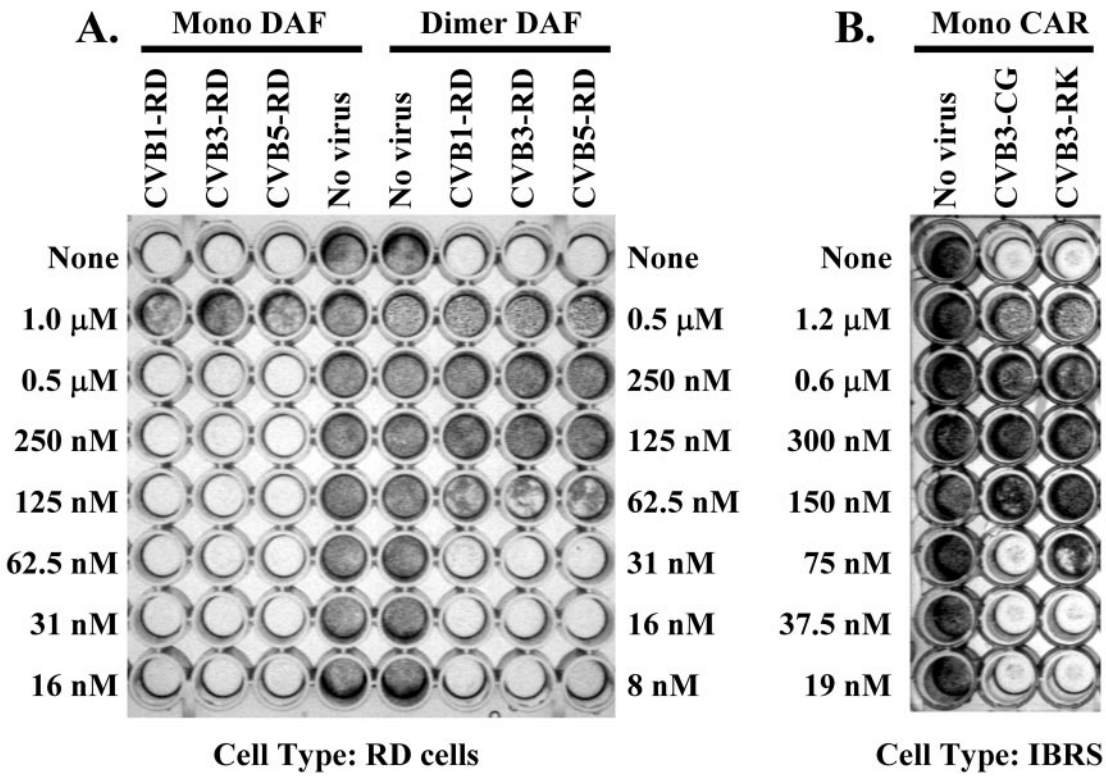

FIG. 1. Inhibition of CVB strains by preincubation with soluble receptors. Representative assay showing inhibition of viral infection (the surviving cell layer is visible as gray) for IBRS cells (B) or RD cells (A) following preincubation of cardiopathogenic CVB3 strains CG or RK with monomeric soluble CAR or RD-adapted CVB serotypes 1, 3, and 5 with monomeric DAF or DAF-Fc, respectively. The top row represents virus infection of cells in the absence of inhibitor, while a fivefold dilution of monomeric DAF (1.0 μM to 16 nM) or dimeric DAF-Fc (0.5 μM to 8 nM) (A) or monomeric CAR (1.2 μM to 19 nM) (B), the former two proteins kept at a molar equivalence for each row. For a complete summary of all viruses, cell types, and Fc-fusion proteins, see Table 1. Final concentrations of soluble receptors are shown at the edge of the plate for all receptors.

them at a concentration of 10^9 cells/ml; then C1 was added to 10^{10} cells dropwise to a final concentration of 5 μg/ml and the mixture was incubated with agitation for 20 min at 30°C. EAC1 cells were washed twice with ice-cold buffer, resuspended to the original volume, and incubated with agitation for 20 min at 30°C with 1 μg/ml of C4. The resultant EAC14 cells were incubated in $DGVB^{++}$ containing C2 (5 μg/ml) for 5 min at 30°C to allow formation of C3 convertase. The cells were then placed on ice for 1 min, centrifuged, and resuspended in prewarmed (30°C) $DGVB^{++}$. An equal volume of these EAC142 cells was added to a range of dilutions of monomeric DAF or DAF-Fc (in $DGVB^{++}$) and allowed to incubate at 30°C with constant shaking for 5 min. One-hundred-microliter aliquots of each sample were removed and added to 100 μl of guinea-pig serum diluted 1:50 in 40 mM EDTA-GVB, and the resultant erythrocyte lysis was determined following incubation at 37°C for 60 min. The amount of released hemoglobin was directly proportional to the residual C3 convertase activity remaining on the EA142 cells and was measured at 405 nm in the supernatant after the unlysed cells were pelleted by centrifugation at 1,000 × *g* for 4 min. Purified C4BP was used as a positive control in these experiments, and all inhibitors were compared to the amount of lysis observed in the absence of added inhibitors.

SPR. The interaction of DAF and CAR in both monomeric and dimeric forms with CVB3-RD and CVB3-GC was analyzed by using SPR (Biacore 2000, Biacore, Sweden). 160S virus particles were purified from the supernatant of infected cells by polyethylene glycol 8000 precipitation and separation by sucrose gradient as detailed above. Peak fractions containing 160S particles were pelleted in a benchtop ultracentrifuge at 40,000 × *g* overnight (8°C) and resuspended in PBS. Four flow cells of a CM5 sensor chip were activated, each with 20 μl of a mixture of 0.2 M 1-ethyl-3-(3 dimethylaminopropyl) carbodiimide and 0.05 M *N*-hydroxy-sulfosuccinimide at a flow rate of 5 μl/min, after which purified CVB strains (in 10 mM Na acetate buffer, pH 4.5) were injected over one flow cell each to reach 650 resonance units (RU) in the case of CVB3-RD and two different densities for CVB3-GC (3,400 and 1,500 RU). Nonutilized reactive groups were blocked with 20 μl of 1 M ethanolamine, pH 8.5. A negative control was prepared by activating and subsequently blocking the surface of flow cell 1. The association kinetics were studied for various concentrations of purified DAF and CAR dialyzed into 10 mM HEPES-KOH, pH 7.4, supplemented with 150 mM NaCl, 3.4 mM EDTA, and 0.005% Tween 20. Protein solutions were injected for 140 s during the association phase at a constant flow rate of 30 μl/min. The sample was injected first over the negative control surface and then over immobilized CVB3 strains. Signal (nonspecific binding and changes in refractive index due to the presence of protein) from the control surface was subtracted. The dissociation was followed for 500 s at the same flow rate. For analyses of DAF-CVB interactions, the sensograms returned to baseline within the 500 s; however, for analyses of CAR binding kinetics, 10 μl of 2 M NaCl–100 mM HCl (pH = 2.5) was required to remove bound ligands during a regeneration step. BiaEvaluation 3.0 software was used to analyze sensograms obtained and to calculate rate affinity constants.

RESULTS

Inhibition of CVB infection by soluble CVB receptors. We measured the viral titers of RD-adapted isolates of CVB serotypes 1, 3, and 5 following preincubation with soluble recombinant monomeric DAF or dimeric DAF-Fc (Fig. 1A). The amount of DAF required to inhibit infection of RD cells was titrated by preincubation of CVB-RD with a fivefold dilution series from 1.0 μM monomeric DAF or 0.5 μM DAF-Fc. For each dilution in these experiments, we used half the molar

TABLE 1. Infection of cell lines by CVB3 stains and inhibition with soluble receptors[a]

Cell line inhibitor	Result for:											
	RD			HuFF			HeLa			IBRS		
	None	DAF-Fc	CAR-Fc	None	DAF-Fc	CAR-Fc	None	DAF-Fc	CAR-Fc	None	DAF-Fc	CAR-Fc
CVB3-CG	NL	—	—	NL	—	—	10^7	10^7	10^0	10^4	10^2	NL
CVB3-RK	NL	—	—	NL	—	—	10^5	10^5	10^1	10^5	10^2	NL
CVB3-RD	10^5	10^3	10^6	10^7	10^3	10^7	10^3	10^3	10^3	10^3	10^2	NL
CVB3-H	10^2	10^1	10^3	10^3	10^1	10^3	10^6	10^5	10^3	10^5	10^1	NL

[a] Representative results for several repeated assays are shown. The amount of infectious virus as identified by lysis of the cell layer is shown. The relative changes of infectivity in the presence of CAR-Fc or DAF-Fc compared to controls were identical between all replications of this experiment. NL, no lysis; —, blocking studies not performed due to inability to lytically infect these cells.

concentration of dimeric DAF (DAF-Fc) to keep the valency of CVB binding sites equivalent to that of monomeric DAF. Monomeric DAF blocked infection only at the highest concentration tested, whereas DAF-Fc inhibited at higher dilutions and was found to be 125-fold-more effective at blocking all serotypes of CVB-RD (Fig. 1A). Since the monomeric DAF and DAF-Fc were produced by different biosynthetic methods (yeast expression versus expression in CHO cells) for these studies, we examined whether the method of recombinant protein production had any influence on the ability of these proteins to inhibit virus infection. We found that monomeric DAF released from DAF-Fc by papain cleavage and purified from contaminants was equivalent in its ability to inhibit CVB infection compared to monomeric DAF produced from *Pichia pastoris* (data not shown).

We next investigated the ability of DAF-Fc to inhibit the cardiopathogenic CVB3 strains CG and RK (Table 1). Neither of these strains caused cytopathic effects in RD cells or primary human fibroblasts (HuFF) due to the absence of cell surface CAR expression (Table 2); however, both CVB3-CG and CVB3-RK readily infected HeLa cells (Table 1) which expressed high levels of both DAF and CAR (Table 2). DAF-Fc caused no block of infection of HeLa cells for either cardiopathogenic strain and also failed to inhibit the limited HeLa cell infection by CVB-RD (Table 1). The pig kidney cell line (IBRS) was permissive for all of the CVB3 strains tested, and we have previously shown that infection is via the pig homologue of CAR (37). Preincubation of virus with DAF-Fc inhibited IBRS cell infection by all CVB3 strains by 10 to 10,000 fold (Table 1). These data suggest that the inhibition of CVB infection by DAF-Fc occurred via steric hindrance of the CAR binding site of the capsid as it blocked infection of CAR-positive, DAF-negative (IBRS) cells.

The ability of soluble recombinant CAR to block infection of cells was also assessed by preincubation of virus with CAR prior to addition to cells (Table 1; Fig. 1B). Monomeric CAR was generated from CAR-Fc by papain cleavage and purified from uncleaved CAR-Fc and the Fc fragments using protein A. Unlike our findings for soluble DAF, monomeric CAR and dimeric CAR-Fc were equally capable of blocking CVB3-CG and CVB3-RK strain infection (data not shown). CAR-Fc blocked CVB3-RD infection of IBRS cells but not infection of HeLa cells, RD cells, or fibroblasts (Table 1). Therefore, CAR-Fc was only able to inhibit CVB3-RD infection of cells that did not express DAF (Tables 1 and 2).

TABLE 2. Flow cytometric assessment of CAR and DAF expression on cell lines[a]

Expression	Cell line			
	HeLa	RD	HuFF	IBRS
Isotype control	18.0 ± 1.0	13.8 ± 17.0	23.6 ± 7.1	4.2 ± 0.3
Anti-human CAR	531 ± 81.0	13.9 ± 1.2	21.0 ± 2.6	194.4 ± 3.0
Anti-human DAF	5,818 ± 595	247.6 ± 17.0	330.7 ± 9.5	4.3 ± 0.5

[a] Values indicate mean cell fluorescence (with standard deviations) for determinations made in triplicate, conducted on three separate days.

Inhibition of complement by soluble DAF. The ability of soluble monomeric DAF and DAF-Fc to regulate complement activation was also assessed. DAF regulates complement activation by accelerating the decay of C3 convertases. Convertase-bearing cells were assembled by sequential addition of purified complement components to antibody sensitized target sheep erythrocytes. We found that fourfold-more DAF-Fc (based on protein molarity) was required to provide the same protection of sheep erythrocytes from complement-mediated lysis compared to monomeric DAF (Fig. 2). On a molar ratio, DAF-Fc contains twice the number of functional sites as monomeric DAF; this means that an 8-to-1 ratio of functional sites between DAF-Fc and monomeric DAF was required to achieve equivalent complement regulation. This suggests that while the dimeric form enhances binding to CVB, this confor-

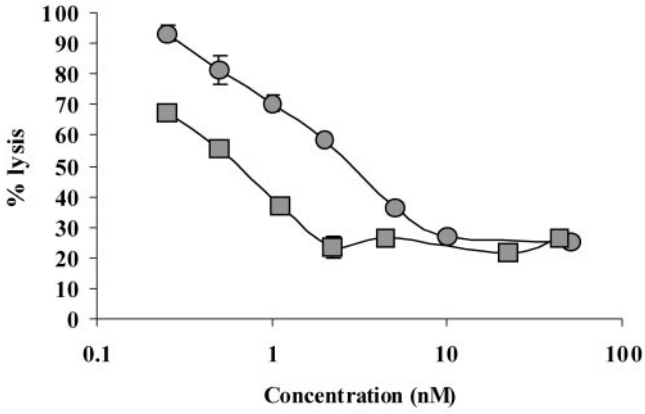

FIG. 2. Comparison of classical C3 convertase decay acceleration by monomeric DAF (squares) or dimeric DAF-Fc (circles). All assays were performed in triplicate, and analyses were repeated at least twice. Error bars represent standard deviations, and 100% lysis refers to the lysis without addition of inhibitor.

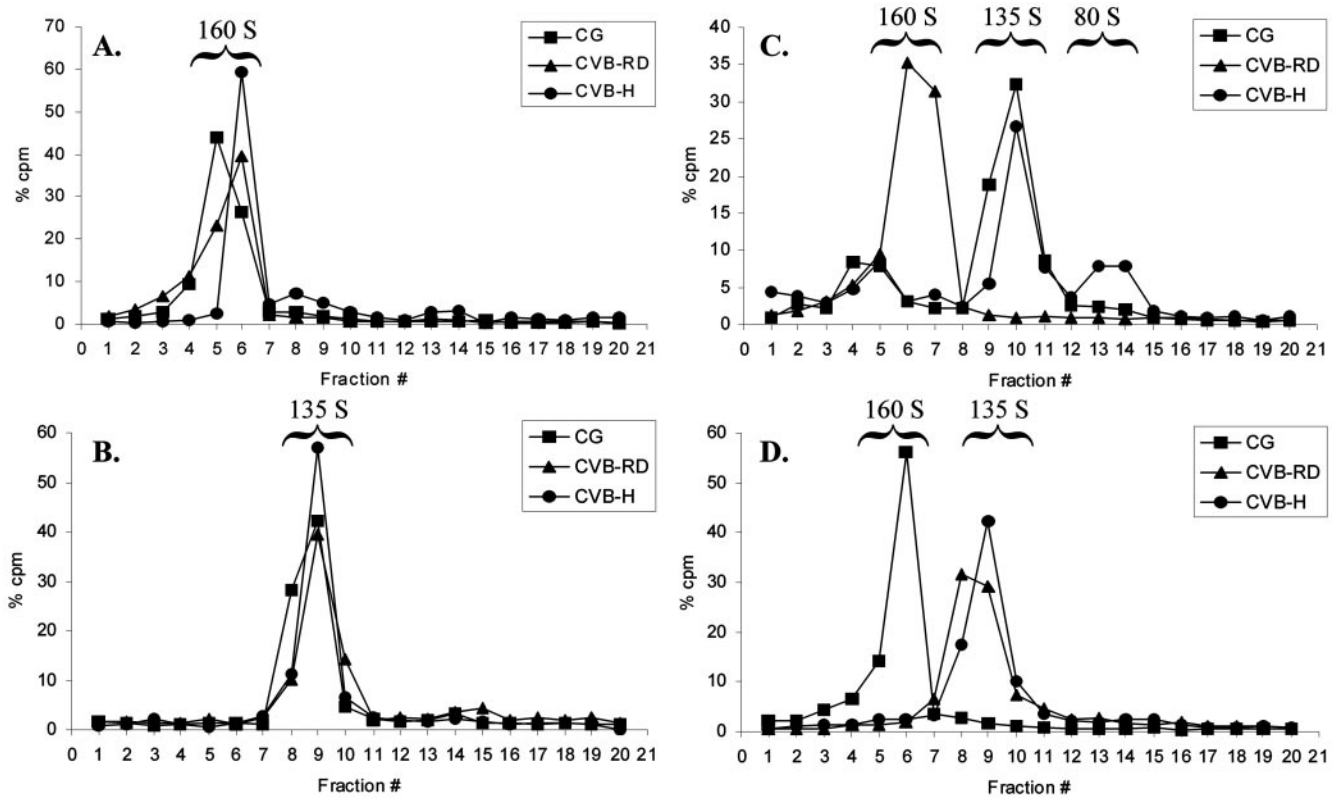

FIG. 3. Separation of full capsids (160S), A particles (135S), and empty capsids (80S) by centrifugation through a 10 to 25% sucrose gradient. Radiolabeled viruses were bound to permissive cells, 0.6 μM DAF-Fc, or CAR-Fc or added to cell medium (control) and rotated for 2 h at 37°C, before cells or particulate debris was removed by centrifugation and loaded onto a sucrose gradient. Fractions (0.5 ml) as taken from the bottom of the gradient to the top are shown for CVB3-CG (squares), CVB3-RD (triangles), or CVB3-H (circles) and plotted as the percent radioactivity of the total loaded on the gradient. (A) Virus incubated with cell medium only; (B) virus eluted from permissive cells; (C) virus incubated with CAR-Fc; (D) virus incubated with DAF-Fc.

mation interferes with the ability of DAF to regulate complement. We have previously shown that CAR does not regulate complement (35).

Readaptation of the CVB3-RD strain to HeLa cells. CVB3-RD did not grow well in HeLa cells (Table 1). However, by inoculating HeLa cells at a multiplicity of infection of 0.1, followed by two serial passages, we selected a variant population with an enhanced capacity to replicate in this cell type. This strain, designated CVB3-H, grew to a higher titer in HeLa cells and had a decreased ability to grow in RD and HuFF cells by 10^3 to 10^4 fold (Table 1). It is interesting that CVB3-H infection of HeLa and IBRS cells was blocked by CAR-Fc, but the residual ability to infect RD cells and HuFF was not (Table 1). CVB3-H also retained the ability to be inhibited by DAF-Fc, as was the parent strain, in HuFF, RD, and IBRS cells. Therefore, CVB3-H was also included in our further studies as it combined the cell tropism and inhibition characteristics of the other three virus strains.

Sucrose gradient separation of CVB3 following incubation with soluble receptors. Radiolabeled 160S CVB3-CG, CVB3-RD, and CVB3-H particles (Fig. 3A) were incubated with either DAF-Fc, CAR-Fc, permissive cells, or cell medium on ice for 1 h, followed by rotation at 37°C for 2 h, and then analyzed for conversion from mature infectious particles (160S) to A particles (135S) or empty capsids (80S) (Fig. 3). CVB3 strains bound to permissive cells and then eluted from the cell surface by incubation at 37°C for 2 h (cells were removed by centrifugation prior to being loaded onto the gradient) served as the positive control for production of A particles (see below and Fig. 3B). Incubation of CVB3-CG and CVB3-H strains, but not the CVB3-RD strain, with CAR-Fc resulted in a decreased sedimentation rate in the gradient, consistent with the formation of A particles (Fig. 3C). Decreased sedimentation was also observed for CVB3-CG, following incubation with CAR-Fc on ice or at room temperature for 2 h (data not shown). No alteration was observed when CVB3-CG was incubated with DAF-Fc (Fig. 3D); however, decreased sedimentation was observed when both CVB-RD and CVB-H were incubated with DAF-Fc (Fig. 3D).

Determination of A particles formation by loss of VP4. The formation of A particles is irreversible, partly due to the externalization and loss of VP4, an internal capsid protein (11). We therefore compared the input and eluted radiolabeled virus particles for the presence of VP4 to confirm that the 135S particles we observed were A particles (Fig. 4). VP4 was absent from all radioactive peaks eluted from permissive cells, which was included as the control for A-particle formation (Fig. 3B and 4). Despite the evidence of altered sedimentation described above for CVB-RD and CVB-H after incubation with DAF-Fc (Fig. 3D), VP4 was retained in the peak radioactive

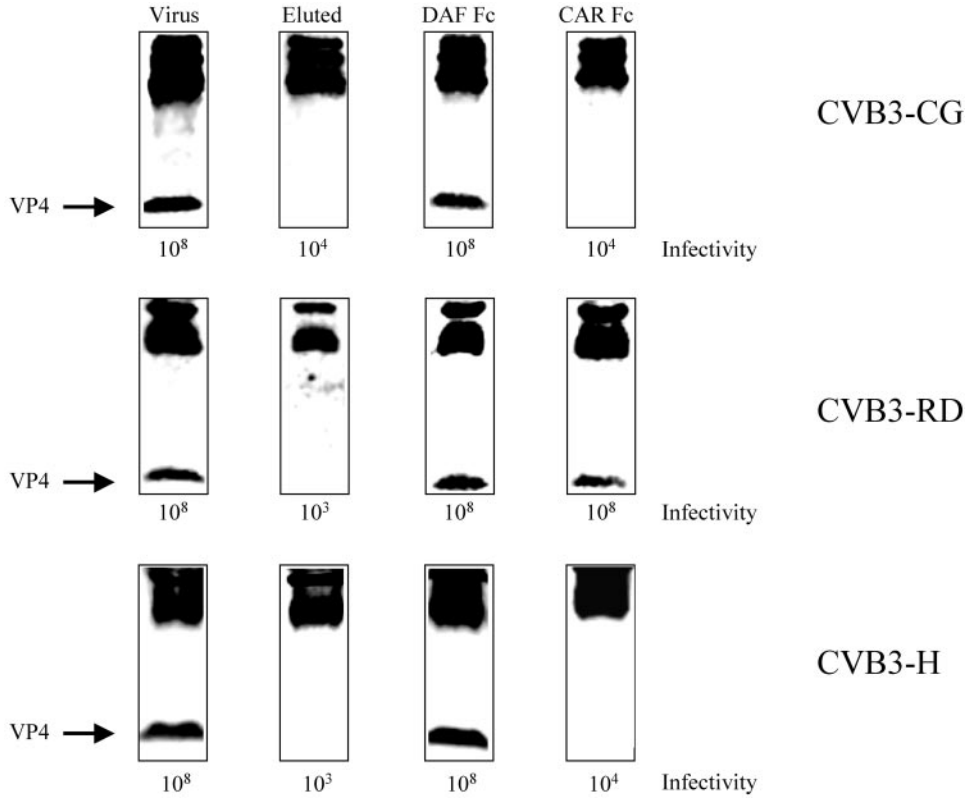

FIG. 4. Autoradiography of CVB3 capsid proteins from peak radioactive fractions, following sucrose gradient separation. Peak fractions following incubation with cell medium only (control) or elution from permissive cells, DAF-Fc, or CAR-Fc were precipitated with trichloroacetic acid and analyzed by Tricine gel electrophoresis. One-hundred-microliter aliquots of these fractions were also dialyzed and assayed for infectivity on permissive cells, and these values ($TCID_{50}$) are listed below the relevant fractions.

fractions, indicating that the altered mobility was caused by stable formation of virus complexes with soluble receptor, rather than the formation of A particles (Fig. 4). In contrast, no VP4 was present for CVB3-CG or CVB-H following incubation with CAR-Fc, confirming the formation of A particles (Fig. 4). It is important to note, however, that even though sedimentation was decreased for CVB3-CG incubated with CAR-Fc on ice and at room temperature, VP4 was retained for both of these conditions (data not shown), indicating that the formation of A particles requires a shift to physiological temperature and that CVB-CAR-Fc can form complexes that impede sedimentation in the gradient.

Recovery of infectious virus from peak radioactive sucrose gradient fractions. One-fifth of each of the peak radioactive fractions shown in Fig. 3 was dialyzed against PBS to remove the sucrose and then used to infect permissive cells. The virus titer, shown as $TCID_{50}$ per milliliter, is indicated below each fraction in Fig. 4. A particles eluted from the cell surface showed a 10^4- to 10^5-fold decrease in infectivity (based on similar amounts of radioactivity present) when compared to virus that was mixed with cell medium alone, similar to that observed for poliovirus neutralization by soluble poliovirus receptor (12, 21). In all cases where viruses showed a loss of VP4, they also had a decreased infectivity consistent with A-particle formation. However, in the case where CVB-RD and CVB-H had been incubated with DAF-Fc, which showed an altered sedimentation but no loss of VP4 (Fig. 3D), the recovered virus was as infectious as the virus control, indicating that an uncoating event had not occurred (Fig. 4).

Measurement of binding affinities of soluble CAR and DAF for CVB3. To assess whether differences in the affinities of soluble CAR and DAF for CVB were responsible for the observed effects on viral infection and stability, we measured binding affinities of the soluble receptors to immobilized CVB by SPR, using methods previously employed for echovirus 11 (EV11) (23). We attempted to immobilize both CVB3-CG and CVB3-RD to a CM5 chip but were unable to immobilize sufficient CVB3-RD to allow confident determination of binding coefficients. Monomeric and dimeric forms of DAF and CAR were dialyzed into standard Biacore analysis buffer (see Materials and Methods), which was of physiological ionic strength, and binding at a range of soluble receptor concentrations was analyzed (Table 3). Sensograms collected for various concen-

TABLE 3. Surface plasmon resonance analysis of soluble receptor affinity for CVB-CG[a]

Analyte	K_D (M)	*ka* (M)	*kd* (M)
Monomeric CAR	2.45×10^{-7}	3.35×10^{3}	8.21×10^{-4}
Dimeric CAR	3.84×10^{-10}	1.62×10^{3}	6.18×10^{-7}
Monomeric DAF	3.82×10^{-4}	NA	NA
Dimeric DAF	1.6×10^{-6}	NA	NA

[a] *kd*, dissociation rate affinity constant; *ka*, association rate affinity constant; NA, not available due to steepness of binding and dissociation curves.

trations of dimeric and monomeric CAR were evaluated by using a 1:1 Langmuir model of binding (Biaevaluation 3.0). Monomeric DAF bound to the CG strain of CVB with the lowest affinity at an equilibrium dissociation constant (K_D) of 3.82×10^{-4} M, while dimeric DAF-Fc bound with an affinity 238-fold higher (1.6×10^{-6} M) (Table 3). The binding of monomeric CAR was 6.5-fold better ($K_D = 2.45 \times 10^{-7}$ M) than the binding of dimeric DAF-Fc, and the dimeric form of CAR, CAR-Fc, resulted in a further 638-fold increase ($K_D = 3.84 \times 10^{-10}$ M) over soluble receptor binding for CVB-CG (Table 3). The lower affinities of DAF than CAR for virus were coupled with on and off rates that were so rapid that it was necessary to calculate the binding affinities by using a steady-state affinity model. When comparing rate affinity constants for monomeric and dimeric CAR, it was apparent that association was not affected by dimerization but that the dimeric protein was dissociating much more slowly than the monomeric CAR. For this reason, a high-salt, low-pH buffer was required to release the bound soluble receptors (see Materials and Methods), while DAF and DAF-Fc completely dissociated under normal flow conditions. Analysis of DAF-Fc binding to CVB-CG performed before and after CAR-Fc binding analysis gave equivalent results, confirming that the regeneration step required for monomeric CAR and CAR-Fc did not alter the binding characteristics of immobilized CVB3-CG (data not shown).

We did attempt to determine if binding of one protein interfered with the binding of the other. Due to the almost immediate dissociation of monomeric DAF and DAF-Fc, it was impossible to preload the immobilized CVB virions and subsequently measure CAR binding. Immobilized CVB (2,000 RU) was preloaded with 0.2 mg/ml CAR-Fc (addition of a further 200 RU), and no subsequent binding of monomeric DAF or DAF-Fc was detectable, although monomeric DAF did bind once the CAR-Fc was removed via a regeneration step. This indicates that binding of the Fc-fusion forms of these proteins can interfere with binding of the other protein; however, we were unable to determine if monomeric forms of both proteins can concurrently bind to the virus.

DISCUSSION

We have previously investigated the ability of DAF-Fc and CAR-Fc to inhibit CVB3-mediated disease in mice (43, 44). We administered either DAF-Fc (43) or CAR-Fc (44) by an intravenous route while infecting the mice with the cardiopathogenic CVB3-CG strain by the intraperitoneal route. While we found that both CAR-Fc and DAF-Fc could abrogate CVB-mediated myocarditis, only CAR-Fc blocked the development of CVB-mediated pancreatitis, suggesting that it had additional effects on the virus. Here, we investigated the basis for these differences, using the same strain of CVB3 and soluble decoy receptors. The in vivo experiments utilized Fc fusion forms of DAF and CAR, primarily to enhance the half-life of the proteins in circulation (30) and to aid purification; however, we expanded our in vitro analysis to compare monomeric and Fc-fusion forms of DAF and CAR. During our investigations, we also noted that infection of CVB3-CG was only weakly susceptible to inhibition by DAF-Fc; therefore, we also included RD-adapted strains of CVB to more fully investigate the potential of DAF-CVB interactions.

We found that DAF-Fc was much better at inhibiting infection by RD-adapted strains of CVB1, 3, and 5 than monomeric DAF (Fig. 1). DAF-Fc also inhibited infection by cardiopathogenic CVB strains CG and RK of cells that lacked endogenous human DAF expression (IBRS cells) (Table 1), an effect that was lost when these cells were transfected with human DAF cDNA (data not shown). These data suggested that inhibition of infection by DAF-Fc was a reversible stearic event; this was confirmed by the demonstration that DAF-Fc failed to induce A-particle formation and virus neutralization (Fig. 4). The observed effective inhibition of CBV-CG infection of mice by DAF-Fc fits this scenario, since we have previously shown that the mouse homologue of DAF is unable to bind CVB (36).

The enhanced CVB inhibition of DAF-Fc compared to monomeric DAF correlated with enhanced viral binding affinity, as determined by SPR analysis (Table 3). In contrast, monomeric CAR and CAR-Fc showed similar inhibition of cardiopathogenic CVB strain infection, regardless of CAR expression by the cell lines (Tables 1 and 2). This may be explained in part by differences in affinity. Both monomeric and dimeric CAR bound virus with an affinity higher than that of DAF-Fc, the latter 10^4-fold higher (Table 3). Our measured affinity for monomeric CAR binding to CVB3 (2.45×10^{-7} M) was lower than the affinity for monomeric CAR and fiber knobs from adenovirus serotypes 5, 12, and 41L (1.5×10^{-9} to 7.9×10^{-9} M) reported by Kirby et al. (22) but higher than their binding affinity of CAR for adenovirus serotype 9 (6.4×10^{-6} M). The binding affinity between CAR and CVB that we measured is similar to values previously found for Ig superfamily virus receptors that bind and induce A-particle formation of other picornaviruses; namely, poliovirus and its receptor (1.1 to 2.3×10^{-7} M), as well as human rhinovirus types 3 or 16 and intercellular adhesion molecule 1 (2.1×10^{-7} to 3.1×10^{-7} M) (26, 42). However, whether the nature of protein binding within the picornavirus capsid canyon structures promotes high-affinity binding or whether high-affinity binding is a requisite for induction of altered capsid conformation has not yet been determined. We were unable to immobilize CVB-RD in sufficient quantities for SPR analysis; however, infection studies showed that CAR-Fc inhibited CVB3-RD infection of DAF-negative IBRS cells but not CAR-negative RD cells. It is important to note, however, that adaptation of CVB strains to lytic growth in RD cells is an artifact of laboratory virus propagation accompanied by increased ability to bind DAF (reference 31 and our unpublished observations). Although Shafren et al. (34) reported that lytic infection of RD cells required the presence of low levels of CAR on these cells, our flow cytometry analysis found negligible CAR expression with both RD cells and human fibroblasts (Table 2). Moreover, infection of RD cells by our CVB-RD strain could not be inhibited by incubation with CAR-Fc. This implies that our CVB-RD strain may be capable of truly CAR-independent infection, analogous to the intercellular adhesion molecule 1-independent, DAF-dependent infection of RD cells, as recently demonstrated by Newcombe et al. (28).

Expression of DAF alone is not sufficient to mediate lytic infection, as CVB-RD cells will not lytically infect CHO cells expressing human DAF (5, 31), while nonadapted CVB strains

will lytically infect CHO cells expressing CAR (25, 31). These data suggest that RD-adapted CVB strains may have adapted to utilize a novel as-yet-unidentified receptor present on RD cells and human fibroblasts in addition to DAF. If so, it is likely that the virus has only low affinity for this additional receptor, as the low-affinity interaction with exogenous soluble DAF is sufficient to block the interaction and prevent infection. It is also interesting that CVB3-RD has been reported to be nonpathogenic in mice (32).

Although dimerization of DAF caused a 100-fold increase in binding affinity for CVB, this was not the case for its ability to inhibit complement. DAF-Fc was fourfold-less effective on a molar basis in inhibiting complement than the monomeric protein. This is in agreement with a previous report examining steric hindrance of complement regulation in DAF-Fc proteins (15). The data suggest that the regions of DAF that regulate complement and those that bind CVB may overlap but also have unique regions as well, similar to that previously shown for echoviruses (41). These conclusions are also supported by differences in binding of anti-DAF monoclonal antibodies or molecularly altered forms of DAF that block complement regulation but not CVB binding, and vice versa (5, 10, 33).

A particles are considered to be an important intermediate in the uncoating events that result in the delivery of the RNA genome to the cell cytoplasm (1, 2), and incubation of poliovirus with soluble poliovirus receptor induces A-particle formation (13, 21, 40). CAR-Fc, unlike DAF-Fc, induced A-particle formation for CVB (Fig. 4). The formation of A particles has been noted for CVB3 eluted from permissive HeLa cells: these particles had a buoyant density of 135S compared to 160S and were missing the smallest capsid protein, VP4 (11). CAR-Fc induction of A-particle formation induced an irreversible loss in infectivity when incubated at 37°C. Although DAF-Fc formed stable complexes with CVB-RD and CVB-H strains capable of remaining intact through a sucrose gradient (Fig. 3D), no A-particle formation was observed (Fig. 4). The ability to induce an irreversible conformation change in the capsid likely contributes to the capacity of CAR-Fc to decrease pathology in CVB-infected mice (44).

In addition to affinity differences, it is likely that the formation of A particles by CAR-Fc but not DAF-Fc involves differences in the capsid binding site for these proteins. The CAR-specific formation of A particles supports the hypothesis that canyon binding receptors are required for uncoating. The canyon is formed primarily by VP1 with a contribution of the hypervariable "puff" region of VP2, and He et al. have localized the CAR binding footprint to this area (17). While no direct structural analysis of CVB-DAF complexes has been performed to date, extrapolations can be made from the cryo-electron microscope reconstruction of echovirus (EV) 7-DAF complexes (18) or EV12-DAF complexes (6), which revealed DAF binding along the twofold axis of symmetry on the EV capsid. Modeling of capsid mutations in echovirus 11 strains that had lost DAF binding suggested that DAF bound at the platform surrounding the fivefold axis of symmetry (38). Both of these putative binding sites are distant from the canyon and may explain the inability of DAF to induce A-particle formation.

A recent report investigated the cellular localization of CAR, DAF, and CVB, following infection of a pancreatic cell line with CVB serotype 4 (39). Following CVB4 binding, virus did not enter via the clathrin-coated pit entry route, where CAR was predominantly found in the absence of viral infection, but colocalized with both DAF and CAR and moved en bloc to the *cis*-Golgi. These results indicate that although DAF and CAR may be associated with distinct physiological pathways within the cell, they traffic synchronously once associated with CVB. These findings imply that DAF does not simply act to sequester the virions for interactions with additional internalizing receptors but may be an important part of targeting the virus to the site of replication during entry, hence explaining the wide range of picornaviruses that interact with this receptor and perhaps making sense of the differing affinities that the two receptors have for the virus.

Concurrent with the submission of the manuscript, Milstone et al. (27) published findings similar to those reported here. They similarly investigated the mechanism behind the inability of DAF expression to mediate permissive infection of transfected CHO cells, which are in contrast to CHO cells expressing CAR. They also examined the ability of soluble and cell-associated CAR to induce CVB A-particle formation. We have expanded on their studies by investigating further strains of CVB3 and provide more extensive investigation of binding affinities of DAF and CAR binding through SPR analysis. Although our findings for RD-adapted CVB3 differ somewhat from theirs, a single passage of our CVB-RD in HeLa cells generated a phenotype equivalent to their CVB-RD. Sequence comparison of the CVB-RD strains from both laboratories may provide additional insight into the CAR binding site for this virus.

ACKNOWLEDGMENTS

This work was funded as part of Career Development Fellowships by the Wellcome Trust (O.B.S. and I.G.G.), the British Heart Foundation (PG/03/111/16032 to O.B.S.), and the Medical Research Council, United Kingdom (G9901250 to D.J.E.), and the Swedish Research Council (A.M.B.).

REFERENCES

1. **Belnap, D. M., D. J. Filman, B. L. Trus, N. Cheng, F. P. Booy, J. F. Conway, S. Curry, C. N. Hiremath, S. K. Tsang, A. C. Steven, and J. M. Hogle.** 2000. Molecular tectonic model of virus structural transitions: the putative cell entry states of poliovirus. J. Virol. **74:**1342–1354.
2. **Belnap, D. M., B. M. McDermott Jr., D. J. Filman, N. Cheng, B. L. Trus, H. J. Zuccola, V. R. Racaniello, J. M. Hogle, and A. C. Steven.** 2000. Three-dimensional structure of poliovirus receptor bound to poliovirus. Proc. Natl. Acad. Sci. USA **97:**73–78.
3. **Bergelson, J. M., J. A. Cunningham, G. Droguett, E. A. Kurt-Jones, A. Krithivas, J. S. Hong, M. S. Horwitz, R. L. Crowell, and R. W. Finberg.** 1997. Isolation of a common receptor for coxsackie B viruses and adenoviruses 2 and 5. Science **275:**1320–1323.
4. **Bergelson, J. M., J. F. Modlin, W. Wieland-Alter, J. A. Cunningham, R. L. Crowell, and R. W. Finberg.** 1997. Clinical coxsackievirus B isolates differ from laboratory strains in their interaction with two cell surface receptors. J Infect. Dis. **175:**697–700.
5. **Bergelson, J. M., J. G. Mohanty, R. L. Crowell, N. F. St John, D. M. Lublin, and R. W. Finberg.** 1995. Coxsackievirus B3 adapted to growth in RD cells binds to decay-accelerating factor (CD55). J. Virol. **69:**1903–1906.
6. **Bhella, D., I. G. Goodfellow, P. Roversi, D. Pettigrew, Y. Chaudhry, D. J. Evans, and S. M. Lea.** 2004. The structure of echovirus type 12 bound to a two-domain fragment of its cellular attachment protein decay-accelerating factor (CD 55). J. Biol. Chem. **279:**8325–8332.
7. **Carson, S. D., and N. M. Chapman.** 2001. Coxsackievirus and adenovirus receptor (CAR) binds immunoglobulins. Biochemistry **40:**14324–14329.
8. **Chretien, I., A. Marcuz, M. Courtet, K. Katevuo, O. Vainio, J. K. Heath, S. J. White, and L. Du Pasquier.** 1998. CTX, a Xenopus thymocyte receptor, defines a molecular family conserved throughout vertebrates. Eur. J. Immunol. **28:**4094–4104.

9. **Cohen, C. J., J. T. Shieh, R. J. Pickles, T. Okegawa, J. T. Hsieh, and J. M. Bergelson.** 2001. The coxsackievirus and adenovirus receptor is a transmembrane component of the tight junction. Proc. Natl. Acad. Sci. USA **98:**15191–15196.
10. **Coyne, K. E., S. E. Hall, S. Thompson, M. A. Arce, T. Kinoshita, T. Fujita, D. J. Anstee, W. Rosse, and D. M. Lublin.** 1992. Mapping of epitopes, glycosylation sites, and complement regulatory domains in human decay accelerating factor. J. Immunol. **149:**2906–2913.
11. **Crowell, R. L., and L. Philipson.** 1971. Specific alterations of coxsackievirus B3 eluted from HeLa cells. J. Virol. **8:**509–515.
12. **Curry, S., M. Chow, and J. M. Hogle.** 1996. The poliovirus 135S particle is infectious. J. Virol. **70:**7125–7131.
13. **Fricks, C. E., and J. M. Hogle.** 1990. Cell-induced conformational change in poliovirus: externalization of the amino terminus of VP1 is responsible for liposome binding. J. Virol. **64:**1934–1945.
14. **Hamann, J., B. Vogel, G. M. van Schijndel, and R. A. van Lier.** 1996. The seven-span transmembrane receptor CD97 has a cellular ligand (CD55, DAF). J. Exp. Med. **184:**1185–1189.
15. **Harris, C. L., C. E. Hughes, A. S. Williams, I. Goodfellow, D. J. Evans, B. Caterson, and B. P. Morgan.** 2003. Generation of anti-complement "pro-drugs": cleavable reagents for specific delivery of complement regulators to disease sites. J. Biol. Chem. **278:**36068–36076.
16. **Harris, C. L., O. B. Spiller, and B. P. Morgan.** 2000. Human and rodent decay-accelerating factors (CD55) are not species restricted in their complement-inhibiting activities. Immunology **100:**462–470.
17. **He, Y., P. R. Chipman, J. Howitt, C. M. Bator, M. A. Whitt, T. S. Baker, R. J. Kuhn, C. W. Anderson, P. Freimuth, and M. G. Rossmann.** 2001. Interaction of coxsackievirus B3 with the full length coxsackievirus-adenovirus receptor. Nat. Struct. Biol. **8:**874–878.
18. **He, Y., F. Lin, P. R. Chipman, C. M. Bator, T. S. Baker, M. Shoham, R. J. Kuhn, M. E. Medof, and M. G. Rossmann.** 2002. Structure of decay-accelerating factor bound to echovirus 7: a virus-receptor complex. Proc. Natl. Acad. Sci. USA **99:**10325–10329.
19. **Honda, T., H. Saitoh, M. Masuko, T. Katagiri-Abe, K. Tominaga, I. Kozakai, K. Kobayashi, T. Kumanishi, Y. G. Watanabe, S. Odani, and R. Kuwano.** 2000. The coxsackievirus-adenovirus receptor protein as a cell adhesion molecule in the developing mouse brain. Brain Res. Mol. Brain Res. **77:**19–28.
20. **Hotta, Y., T. Honda, M. Naito, and R. Kuwano.** 2003. Developmental distribution of coxsackie virus and adenovirus receptor localized in the nervous system. Brain Res. Dev. Brain Res. **143:**1–13.
21. **Kaplan, G., M. R. Freistadt, and V. R. Racaniello.** 1990. Neutralization of poliovirus by cell receptors expressed in insect cells. J. Virol. **64:**4697–4702.
22. **Kirby, I., R. Lord, E. Davison, T. J. Wickham, P. W. Roelvink, I. Kovesdi, B. J. Sutton, and G. Santis.** 2001. Adenovirus type 9 fiber knob binds to the coxsackie B virus-adenovirus receptor (CAR) with lower affinity than fiber knobs of other CAR-binding adenovirus serotypes. J. Virol. **75:**7210–7214.
23. **Lea, S. M., R. M. Powell, T. McKee, D. J. Evans, D. Brown, D. I. Stuart, and P. A. van der Merwe.** 1998. Determination of the affinity and kinetic constants for the interaction between the human virus echovirus 11 and its cellular receptor, CD55. J. Biol. Chem. **273:**30443–30447.
24. **Lin, H. H., M. Stacey, C. Saxby, V. Knott, Y. Chaudhry, D. Evans, S. Gordon, A. J. McKnight, P. Handford, and S. Lea.** 2001. Molecular analysis of the epidermal growth factor-like short consensus repeat domain-mediated protein-protein interactions: dissection of the CD97-CD55 complex. J. Biol. Chem. **276:**24160–24169.
25. **Martino, T. A., M. Petric, H. Weingartl, J. M. Bergelson, M. A. Opavsky, C. D. Richardson, J. F. Modlin, R. W. Finberg, K. C. Kain, N. Willis, C. J. Gauntt, and P. P. Liu.** 2000. The coxsackie-adenovirus receptor (CAR) is used by reference strains and clinical isolates representing all six serotypes of coxsackievirus group B and by swine vesicular disease virus. Virology **271:**99–108.
26. **McDermott, B. M., Jr., A. H. Rux, R. J. Eisenberg, G. H. Cohen, and V. R. Racaniello.** 2000. Two distinct binding affinities of poliovirus for its cellular receptor. J. Biol. Chem. **275:**23089–23096.
27. **Milstone, A. M. J. Petrella, M. D. Sanchez, M. Muhmud, J. C. Whitbeck, and J. M. Bergelson.** 2005. Interaction with coxsackievirus and adenovirus receptor, but not with decay-accelerating factor (DAF), induces A-particle formation in a DAF-binding coxsackie B3 isolate. J. Virol. **79:**655–660.
28. **Newcombe, N. G., L. G. Beagley, D. Christiansen, B. E. Loveland, E. S. Johansson, K. W. Beagley, R. D. Barry, and D. R. Shafren.** 2004. Novel role for decay-accelerating factor in coxsackievirus A21-mediated cell infectivity. J. Virol. **78:**12677–12682.
29. **Powell, R. M., T. Ward, D. J. Evans, and J. W. Almond.** 1997. Interaction between echovirus 7 and its receptor, decay-accelerating factor (CD55): evidence for a secondary cellular factor in A-particle formation. J. Virol. **71:**9306–9312.
30. **Powers, D. B., P. Amersdorfer, M. Poul, U. B. Nielsen, M. R. Shalaby, G. P. Adams, L. M. Weiner, and J. D. Marks.** 2001. Expression of single-chain Fv-Fc fusions in Pichia pastoris. J. Immunol. Methods **251:**123–135.
31. **Schmidtke, M., H. C. Selinka, A. Heim, B. Jahn, M. Tonew, R. Kandolf, A. Stelzner, and R. Zell.** 2000. Attachment of coxsackievirus B3 variants to various cell lines: mapping of phenotypic differences to capsid protein VP1. Virology **275:**77–88.
32. **Selinka, H. C., A. Wolde, A. Pasch, K. Klingel, J. J. Schnorr, J. H. Kupper, A. M. Lindberg, and R. Kandolf.** 2002. Comparative analysis of two coxsackievirus B3 strains: putative influence of virus-receptor interactions on pathogenesis. J. Med. Virol. **67:**224–233.
33. **Shafren, D. R., R. C. Bates, M. V. Agrez, R. L. Herd, G. F. Burns, and R. D. Barry.** 1995. Coxsackieviruses B1, B3, and B5 use decay accelerating factor as a receptor for cell attachment. J. Virol. **69:**3873–3877.
34. **Shafren, D. R., D. T. Williams, and R. D. Barry.** 1997. A decay-accelerating factor-binding strain of coxsackievirus B3 requires the coxsackievirus-adenovirus receptor protein to mediate lytic infection of rhabdomyosarcoma cells. J. Virol. **71:**9844–9848.
35. **Spiller, O. B., D. J. Blackbourn, L. Mark, D. G. Proctor, and A. M. Blom.** 2003. Functional activity of the complement regulator encoded by Kaposi's sarcoma-associated herpesvirus. J. Biol. Chem. **278:**9283–9289.
36. **Spiller, O. B., I. G. Goodfellow, D. J. Evans, J. W. Almond, and B. P. Morgan.** 2000. Echoviruses and coxsackie B viruses that use human decay-accelerating factor (DAF) as a receptor do not bind the rodent analogues of DAF. J. Infect. Dis. **181:**340–343.
37. **Spiller, O. B., I. G. Goodfellow, D. J. Evans, S. J. Hinchliffe, and B. P. Morgan.** 2002. Coxsackie B viruses that use human DAF as a receptor infect pig cells via pig CAR and do not use pig DAF. J Gen. Virol. **83:**45–52.
38. **Stuart, A. D., T. A. McKee, P. A. Williams, C. Harley, S. Shen, D. I. Stuart, T. D. Brown, and S. M. Lea.** 2002. Determination of the structure of a decay accelerating factor-binding clinical isolate of echovirus 11 allows mapping of mutants with altered receptor requirements for infection. J. Virol. **76:**7694–7704.
39. **Triantafilou, K., and M. Triantafilou.** 2004. Lipid-raft-dependent coxsackievirus B4 internalization and rapid targeting to the Golgi. Virology **326:**6–19.
40. **Tsang, S. K., B. M. McDermott, V. R. Racaniello, and J. M. Hogle.** 2001. Kinetic analysis of the effect of poliovirus receptor on viral uncoating: the receptor as a catalyst. J. Virol. **75:**4984–4989.
41. **Williams, P., Y. Chaudhry, I. G. Goodfellow, J. Billington, R. Powell, O. B. Spiller, D. J. Evans, and S. Lea.** 2003. Mapping CD55 function. The structure of two pathogen-binding domains at 1.7 A. J. Biol. Chem. **278:**10691–10696.
42. **Xing, L., K. Tjarnlund, B. Lindqvist, G. G. Kaplan, D. Feigelstock, R. H. Cheng, and J. M. Casasnovas.** 2000. Distinct cellular receptor interactions in poliovirus and rhinoviruses. EMBO J. **19:**1207–1216.
43. **Yanagawa, B., O. B. Spiller, J. Choy, H. Luo, P. Cheung, H. M. Zhang, I. G. Goodfellow, D. J. Evans, A. Suarez, D. Yang, and B. M. McManus.** 2003. Coxsackievirus B3-associated myocardial pathology and viral load reduced by recombinant soluble human decay-accelerating factor in mice. Lab. Investig. **83:**75–85.
44. **Yanagawa, B., O. B. Spiller, D. G. Proctor, J. Choy, H. Luo, H. M. Zhang, A. Suarez, D. Yang, and B. M. McManus.** 2004. Soluble recombinant coxsackievirus and adenovirus receptor abrogates coxsackievirus b3-mediated pancreatitis and myocarditis in mice. J Infect. Dis. **189:**1431–1439.